

Geophysical Research Letters®

RESEARCH LETTER

10.1029/2023GL108020

Rapid Ice-Wedge Collapse and Permafrost Carbon Loss Triggered by Increased Snow Depth and Surface Runoff



Key Points:

- A decade of raised snow depths led to strong local thaw subsidence, while increased runoff triggered the downstream collapse of ice wedges
- The abrupt thaw process mobilized about 1.1–3.3 tons of soil organic carbon in total, and dissolved organic carbon was degraded in the thermo-erosion gully
- Feedbacks linking changes in snow cover, surface drainage, and permafrost thaw are important drivers of thermokarst and soil carbon loss

Supporting Information:

Supporting Information may be found in the online version of this article.

Correspondence to:

F.-J. W. Parmentier,
frans-jan@thissideofthearctic.org

Citation:

Parmentier, F.-J. W., Nilsen, L., Tømmervik, H., Meisel, O. H., Bröder, L., Vonk, J. E., et al. (2024). Rapid ice-wedge collapse and permafrost carbon loss triggered by increased snow depth and surface runoff. *Geophysical Research Letters*, 51, e2023GL108020. <https://doi.org/10.1029/2023GL108020>

Received 22 DEC 2023







Accepted 10 APR 2024

Author Contributions:

Conceptualization: Frans-Jan W. Parmentier, Elisabeth J. Cooper
Data curation: Frans-Jan W. Parmentier, Ove H. Meisel, Lisa Bröder, Philipp R. Semenchuk, Elisabeth J. Cooper
Formal analysis: Frans-Jan W. Parmentier, Lennart Nilsen, Hans Tømmervik, Ove H. Meisel, Lisa Bröder, Jorien E. Vonk, Philipp R. Semenchuk, Elisabeth J. Cooper
Funding acquisition: Elisabeth J. Cooper
Investigation: Frans-Jan W. Parmentier, Hans Tømmervik, Jorien E. Vonk, Sebastian Westermann, Elisabeth J. Cooper

© 2024. The Author(s).

This is an open access article under the terms of the [Creative Commons Attribution License](https://creativecommons.org/licenses/by/4.0/), which permits use, distribution and reproduction in any medium, provided the original work is properly cited.

Frans-Jan W. Parmentier¹ , Lennart Nilsen², Hans Tømmervik³ , Ove H. Meisel^{4,5}, Lisa Bröder⁶ , Jorien E. Vonk⁵, Sebastian Westermann¹ , Philipp R. Semenchuk⁷ , and Elisabeth J. Cooper² 

¹Center for Biogeochemistry of the Anthropocene, Department of Geosciences, University of Oslo, Oslo, Norway,

²Department of Arctic and Marine Biology, UiT–The Arctic University of Norway, Tromsø, Norway, ³Norwegian Institute for Nature Research, FRAM - High North Research Centre for Climate and the Environment, Tromsø, Norway, ⁴School of Geographical Sciences, University of Bristol, Bristol, UK, ⁵Department of Earth Sciences, Faculty of Earth and Life Sciences, Vrije Universiteit Amsterdam, Amsterdam, The Netherlands, ⁶Department of Earth Sciences, ETH Zürich, Zürich, Switzerland, ⁷Department of Arctic Biology, UNIS–The University Centre in Svalbard, Longyearbyen, Norway

Abstract Thicker snow cover in permafrost areas causes deeper active layers and thaw subsidence, which alter local hydrology and may amplify the loss of soil carbon. However, the potential for changes in snow cover and surface runoff to mobilize permafrost carbon remains poorly quantified. In this study, we show that a snow fence experiment on High-Arctic Svalbard inadvertently led to surface subsidence through warming, and extensive downstream erosion due to increased surface runoff. Within a decade of artificially raised snow depths, several ice wedges collapsed, forming a 50 m long and 1.5 m deep thermo-erosion gully in the landscape. We estimate that 1.1–3.3 tons C may have eroded, and that the gully is a hotspot for processing of mobilized aquatic carbon. Our results show that interactions among snow, runoff and permafrost thaw form an important driver of soil carbon loss, highlighting the need for improved model representation.

Plain Language Summary Snow cover is steadily disappearing as a result of climate change, but in areas that remain below 0°C we can still expect an increase in snow depth in the middle of winter. Since snow acts akin to a blanket, this warms the soil and accelerates the thaw of permafrost—thereby potentially contributing to carbon release from these frozen soils. Ice wedges, which are typical for permafrost landscapes, are particularly vulnerable to thaw because they hold a large amount of ice. When this ice melts, the surface sinks down, and soil carbon may be lost. In this study, we show how experimentally raised snow cover triggered the collapse of several ice wedges, not only through a warming effect of the snow but also due to an increase in the flow of water through the ice wedge network. As a result, we estimate that 1.1–3.3 tons of carbon were removed from this location, of which a portion could have entered the atmosphere as CO₂. We emphasize the importance of studying the interactions among snow, runoff, and permafrost thaw to better understand how this may affect the release of greenhouse gases to the atmosphere.

1. Introduction

Precipitation is projected to increase across extensive parts of the Arctic (AMAP, 2017) since both enhanced poleward transport and an increasingly sea ice-free Arctic Ocean lead to more atmospheric moisture (Bintanja & Selten, 2014; Zhang et al., 2013). In regions where temperatures remain below 0°C, this will increase mid-winter snowpacks despite an overall warming and shortening of the snow-covered season (Pulliainen et al., 2020). Thicker, insulating snowpacks shield the ground from the coldest winter temperatures, which leads to a net warming of the soil beneath (Stieglitz et al., 2003). In the permafrost region, this causes a thickening of the active layer, and ultimately talik formation if the soil remains unfrozen, which may trigger surface subsidence called thermokarst (Farquharson et al., 2022; Johansson et al., 2013). Thermokarst features such as active layer detachment slides, retrogressive thaw slumps, and thermo-erosion gullies have the potential to mobilize permafrost carbon (Jorgenson & Osterkamp, 2005; Lantuit & Pollard, 2008). How much of the carbon is transported, and possibly released to the atmosphere as greenhouse gases, strongly depends on local hydrological conditions (Liljedahl et al., 2016). It is therefore important to understand how the interplay of snow, water, and permafrost may act as a driver of carbon-climate feedbacks.

Methodology: Frans-Jan W. Parmentier, Lennart Nilsen, Hans Tømmervik, Ove H. Meisel, Lisa Bröder, Jorien E. Vonk, Philipp R. Semenchuk, Elisabeth J. Cooper
Project administration: Lennart Nilsen, Elisabeth J. Cooper
Resources: Frans-Jan W. Parmentier, Hans Tømmervik, Jorien E. Vonk, Philipp R. Semenchuk, Elisabeth J. Cooper
Software: Frans-Jan W. Parmentier, Hans Tømmervik
Validation: Frans-Jan W. Parmentier, Sebastian Westermann, Elisabeth J. Cooper
Visualization: Frans-Jan W. Parmentier
Writing – original draft: Frans-Jan W. Parmentier, Lennart Nilsen, Hans Tømmervik, Ove H. Meisel, Lisa Bröder, Jorien E. Vonk, Sebastian Westermann, Philipp R. Semenchuk, Elisabeth J. Cooper
Writing – review & editing: Frans-Jan W. Parmentier, Lennart Nilsen, Hans Tømmervik, Ove H. Meisel, Lisa Bröder, Jorien E. Vonk, Sebastian Westermann, Philipp R. Semenchuk, Elisabeth J. Cooper

Permafrost environments may be impacted non-uniformly by snow cover changes, given their high heterogeneity. Of the many types of periglacial landscape features, ice wedge landscapes are particularly vulnerable to subsidence due to their high ice content (Jorgenson et al., 2022). Ice wedges form when, year after year, frost cracks fill with melt water in spring and refreeze (Lachenbruch, 1962). The thermal contraction and expansion from numerous freeze-thaw cycles, across centuries to millennia, leads to the development of troughs and elevated rims that connect to form the polygonal patterns characteristic of arctic landscapes. While ice wedges take a long time to form, climate change can degrade them relatively quickly, causing a transition from low to high center polygons (Liljedahl et al., 2016). This enhances surface drainage, concentrating runoff through deepened troughs, and promotes thermal and mechanical erosion. In extreme cases, this causes the collapse of ice wedges (Fortier et al., 2007). An improved understanding of the formation of such thermo-erosion gullies is key to quantify the loss of permafrost carbon due to abrupt thaw.

While only a fifth of the northern permafrost region is susceptible to abrupt thaw processes, these areas hold about half of the total below-ground carbon pool (Olefeldt et al., 2016). For example, ice wedges can represent up to 50% of the volume in carbon-rich Yedoma deposits (Ulrich et al., 2014), and are an important reservoir of biodegradable carbon (Fritz et al., 2015; Vonk, Mann, Dowdy, et al., 2013). Despite the importance of thermokarst for the permafrost carbon feedback, no Earth system model is able to represent this despite recent advances in landscape-scale process models (Aas et al., 2019; Nitzbon et al., 2020). As a result, lateral carbon export from the permafrost region is one of the most uncertain components of the arctic carbon cycle (Turetsky et al., 2020), highlighting the need for more process understanding.

In this study, we investigate the unforeseen side effects of a snow fence experiment on Svalbard. This experiment, consisting of four clusters of three fences each, was originally designed to study the effects of snow cover change on vegetation. However, at one snow fence it inadvertently led to strong surface subsidence and the collapse of ice wedges situated downstream—within a decade from initiation of the experiment (Figure 1). This created a unique opportunity to show—in a controlled setting—how increased snow cover can have both a direct and remote effect on abrupt permafrost thaw and carbon mobilization. We use remote sensing to pinpoint the timing of abrupt thaw, characterize mobilized soil carbon in water samples, and hypothesize how a change in snow cover across a relatively small area triggered the rapid downstream change in the landscape.

2. Methods

2.1. Snow Fence Experiment

Snow fences are practical tools to passively increase snow cover thickness, by decreasing windspeed on their leeward side, and to study subsequent impacts on ecosystems and soils (see e.g., Johansson et al., 2013; Natali et al., 2011; Plaza et al., 2019). The snow fences of this study are placed in the High-Arctic valley of Adventdalen on Svalbard (78°10'N, 16° 06'E). Since 2006, 12 snow fences, each 6.2 m long and 1.5 m high, have been spread out in four groups of three, within ~1 km from each other (Figure S1 in Supporting Information S1). The fences are situated on a slight north-facing slope (<3%), cut by several streams originating from a mountain plateau to the south. This area is characterized by continuous permafrost formed in aeolian deposits on top of alluvial terraces of Holocene age (Gilbert et al., 2018). The varying geomorphology at each snow fence cluster led to a variable potential for surface subsidence. Nine fences (clusters A, B, and D) were in areas with well-drained cryoturbated soils and/or a high boulder content, with low and rather uniform excess ice contents that do not cause strong contrasts in surface subsidence—which is common throughout the valley (Cable et al., 2018). However, the three fences of cluster C were located in a high center polygon field, a feature absent at the other clusters (Figure S1 in Supporting Information S1). The high ice content of these ice wedges mediated subsidence following warming from increased snow cover. Typical snow depth behind the fences is 130 ± 25 cm at the end of the winter, and 32 ± 14 cm for the control plots. Snow accumulates >20 m to the west of the fences, but the greatest depths occur 3–12 m behind the fences (Figure S2 in Supporting Information S1). Compared to the control plots, snow behind the fences is melting 6–14 days later. More details about the experiment are included in Cooper et al. (2011).

2.2. Remotely Sensed Imagery

The snow fence experiment was initiated to study snow-vegetation interactions, and not systematically monitored for indications of abrupt permafrost thaw. Therefore, we use remote sensing to track changes in the landscape. Due to the infrequent overpasses of high resolution satellites (<1 m), combined with prevalent cloud cover and

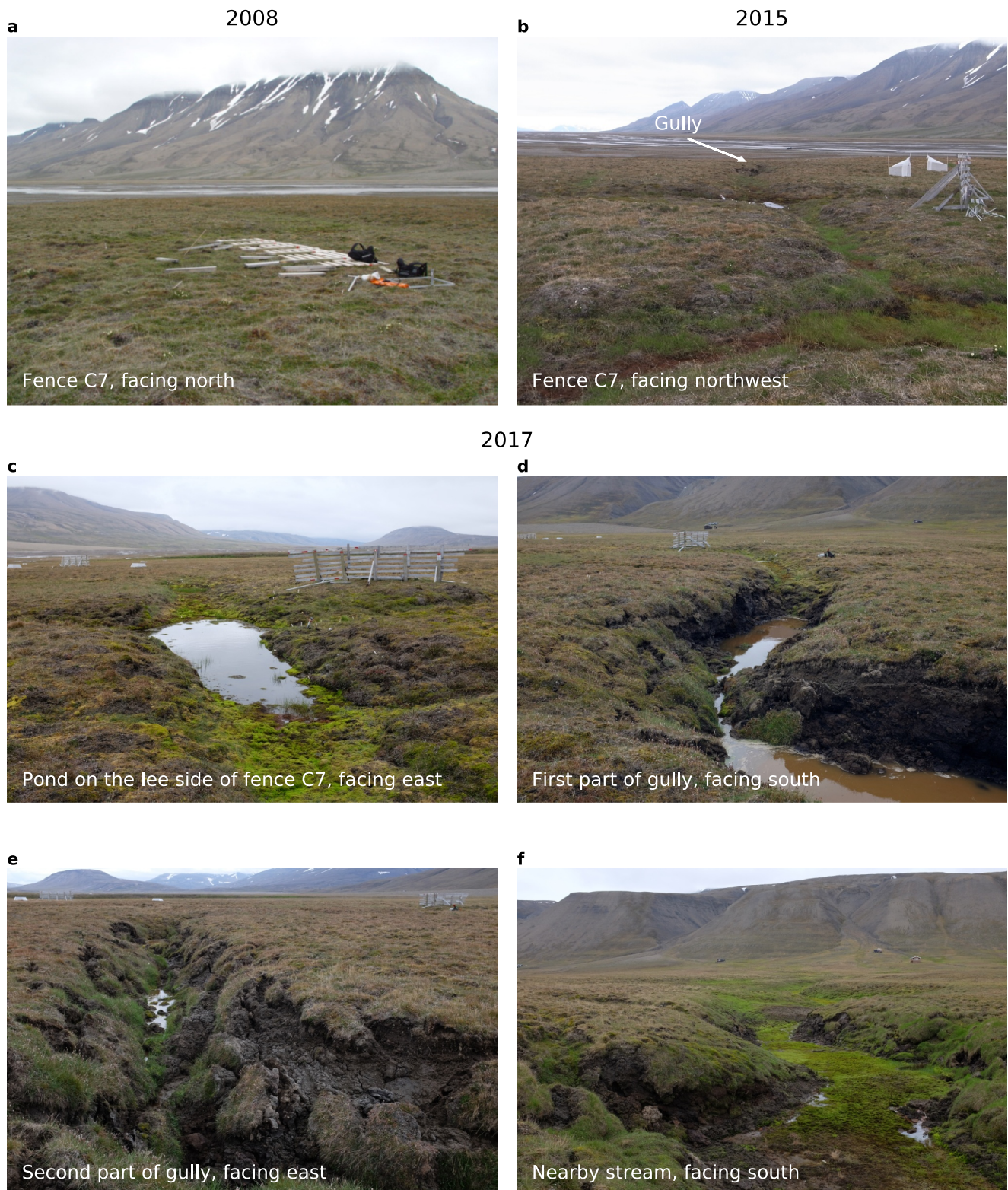


Figure 1. Large downstream effects of increased snow cover. (a) July 2008, showing an undisturbed ground surface. The snow fence was down for repair. (b) July 2015, when ice wedge troughs had deepened. The start of the gully is visible in the background. (c–f) August 2017, showing (c) a deep thaw pond behind the snow fence (d), a deepened trough leading into the gully, (e), the continuation of the same gully. The gullyhead is to the bottom right of this picture. (f) The nearby stream in which the gully exits. The gullyhead is to the left.

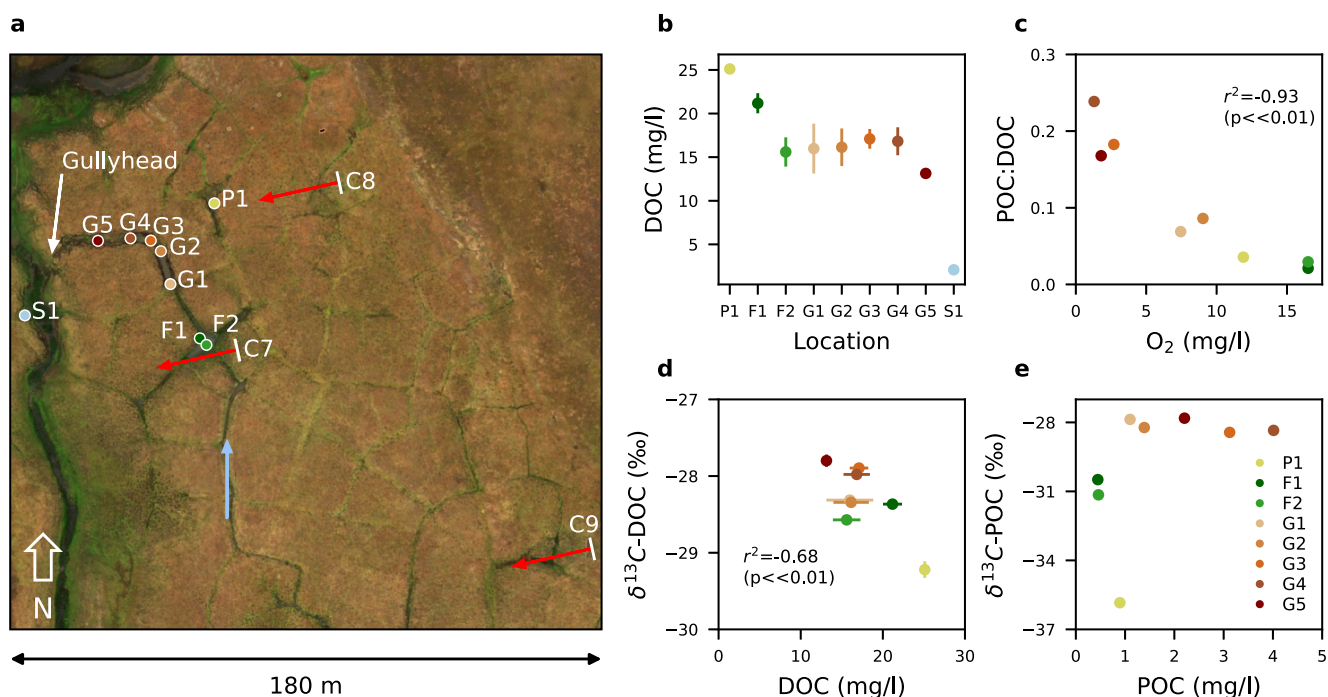


Figure 2. (a) Overview of sample locations and (b–e) water samples analysis. Left: sample locations for a nearby thaw pond (P1), the thaw pond behind fence C7 (F1 and F2), the gully (G1–G5) and a nearby stream for background values (S1). The red arrows extending from the fences (C7–C9) show where snow depth was raised, the light blue arrow indicates the direction of overland flow through ice wedge troughs, the white arrow the gullyhead. (b) Right: scatterplots showing a spatial pattern in dissolved organic carbon (DOC), (c) a strong inverse correlation between POC:DOC and O_2 , (d) an inverse correlation between DOC and $\delta^{13}C\text{-DOC}$, and (e) a clustering for $\delta^{13}C\text{-POC}$. All data are shown in Table S1 in Supporting Information S1.

short snow-free summers on Svalbard, only four high quality images spanned the formation of the thermo-erosion gully: an aerial survey by the Norwegian Polar Institute in 2009 (resolution: ~ 20 cm), and imagery from the Digital Globe constellation of satellites for 2011, 2013, and 2015 (pansharpened to ~ 0.5 m). In addition, we acquired three monochrome Formosat-2 images for 2011 and 2012 (pansharpened to ~ 2 m) and surveyed the area with a MicaSense RedEdge on a drone on 5 September 2017. Further details are in Supporting Information S1.

2.3. Water Sample Analysis

Water samples were collected on 5 and 6 August 2017, from various water features near the snow fence (Figure 2a): one from a natural thaw pond (P1), two samples from the thaw pond behind the affected snow fence (F1 and F2), and five from the water standing still in the gully (G1–G5). As a background signal, we collected a sample from a nearby stream that flows northwards from the mountain to the south, at a point hydrologically isolated from the other locations (S1). These water samples were analyzed for dissolved organic carbon (DOC), particulate organic carbon (POC), particulate nitrogen (PN) content, and stable carbon isotope ratios $\delta^{13}C\text{-DOC}$ and $\delta^{13}C\text{-POC}$. A full description of the analysis is included in Supporting Information S1. Temperature, pH, oxygen, and electrical conductivity were measured in the field on the day of sampling.

3. Results

3.1. Transformation of the Landscape

The snow fence experiment raised soil temperatures by $2\text{--}5^\circ\text{C}$ during the cold season (Semenchuk et al., 2016). Because of this warming, the ice wedges close to the fences of cluster C had developed deep troughs (Figure 1 and Figure S3 in Supporting Information S1), with the largest changes at fence C7. In the summer of 2017, about 10 years after the experiment started, troughs behind this fence were $40\text{--}60$ cm deep as opposed to $20\text{--}30$ cm for unaffected troughs located nearby and upslope from the experiment. At an intersection of several ice wedges, thaw subsidence became so severe that a large pond formed (Figure 1c).

In contrast to previous snow fence experiments, the largest impact of this experiment occurred downstream: a series of ice wedges collapsed 25–75 m away and formed a gully ~1.5 m deep, ~3 m wide, and 50 m long (Figures 1d, 1e, and 2a). This thermo-erosion gully (hereafter gully) exited into a nearby stream, ~5 m lower in the landscape than the top of the polygon centers (Figure 1f).

No runoff was observed during visits in August 2017 and July 2019. The gullyhead had collapsed, causing a barrier to outflow into the stream, and about 20–30 cm of water was standing still on the bottom of the gully. Water primarily flows through this gully around the time of snowmelt, when a large amount of meltwater flows from the upslope area, or in the direct aftermath of rain. Little rain falls on Svalbard but, when showers occur, surface runoff is funneled through the stream channels formed by the polygon troughs (Figure S4 in Supporting Information S1).

3.2. Sudden Collapse of Ice Wedges Detected With Remote Sensing

A timeline of the collapse of the ice wedges was reconstructed with remote sensing. In 2009, after three winters of increased snow depth, no notable change of the ice wedges was detected (Figure 3). Satellite data from 2011 shows that Normalized Difference Vegetation Index (NDVI) is reduced on the leeward side (west) of the snow fences. An increase in snow depth with subsequent delay in snowmelt causes lower live biomass—a feature common to all snow fences (Cooper et al., 2019). A concurrent increase in Normalized Difference Water Index (NDWI) indicates that the soil also became wetter. Photos from an automated camera setup on a nearby mountain (Parmentier et al., 2021) show standing water behind fence C7 for extended periods in August and September 2011, but not yet permanently (Figure S4 in Supporting Information S1).

The most apparent shift occurred between 2011 and 2013 near fence C7 (Figure 3). NDWI strongly increased, while NDVI strongly decreased. The pond behind the fence is clearly visible, and the downstream ice wedges, to the northwest, had collapsed. In 2015, NDWI and NDVI show further shifts along the collapsed ice wedge, as well as a widening of the gully. Large parts of the sides of the gully collapsed in between July and August 2017 (Figure S5 in Supporting Information S1), while a subsequent visit in 2021 did not show much additional collapse (Figure S6 in Supporting Information S1). Meanwhile, lower resolution imagery from Formosat-2 indicates that the gully was already present in 2012 (Figure S7 in Supporting Information S1). This means that gully formation was spread out over several years, with additional soil material entering the gully in the weeks before collection of the water samples.

3.3. Characterization of Water Samples

On average, the water in the gully was colder, more acidic, and lower in oxygen than in the ponds, while containing 4 ± 0.7 times as much POC and 3.4 ± 0.7 times as much PN (Figures 2b–2e, Table S1 in Supporting Information S1). The values for $\delta^{13}\text{C}$ -POC were higher and more consistent in the gully than in the thaw ponds ($-28.3\text{‰} \pm 0.3$ vs. $-32.5\text{‰} \pm 2.9$, respectively). Also, the C:N ratios between the two were different ($p < 0.02$): 9.8 ± 0.7 in the thaw ponds, and 11.8 ± 0.9 in the gully. Soil cores from this area showed C:N ratios of 13.9 ± 2.0 in the top of the active layer and a pH of 5.1 ± 0.3 for pore water (Schostag et al., 2015).

DOC levels in the ponds and the gully were an order of magnitude higher (17.4 ± 4 vs. 2.0 ± 0.5 mg/l) than background values (2 ± 0.5 mg/l) in the nearby stream. The highest values were measured in the natural thaw pond (25.3 ± 0.5 mg/l), and in one of the two samples collected behind the snow fence (21.4 ± 1.2 mg/l). Figure 2b shows that there was a general downward trend in DOC from the thaw ponds (P1, F1, and F2) and further down the gully (G1–G5). Along the same gradient, POC:DOC shows a strong inverse relationship with O_2 (Figure 2c).

3.4. Total Mobilized Soil Carbon

To achieve a rough estimate of the total amount of mobilized soil carbon, we combined the approximate volume of the eroded ice wedge with previously measured soil carbon content from Adventdalen. Samples collected in the upper ~15 cm of soil within the snow fence experiment had average C contents of $41.7\text{--}66$ kg C m^{-3} (Semenchuk et al., 2019) while 1-m-deep soil cores collected from the rims of ice wedges and next to a polygon in Adventdalen show an average carbon content of 33.3 ± 11.2 kg C m^{-3} (Palmtag et al., 2022). The size of the gully was 50 m long, on average 1.5 m deep, 3 m wide at the top, and 1 m wide at the bottom, which translates to a volume of

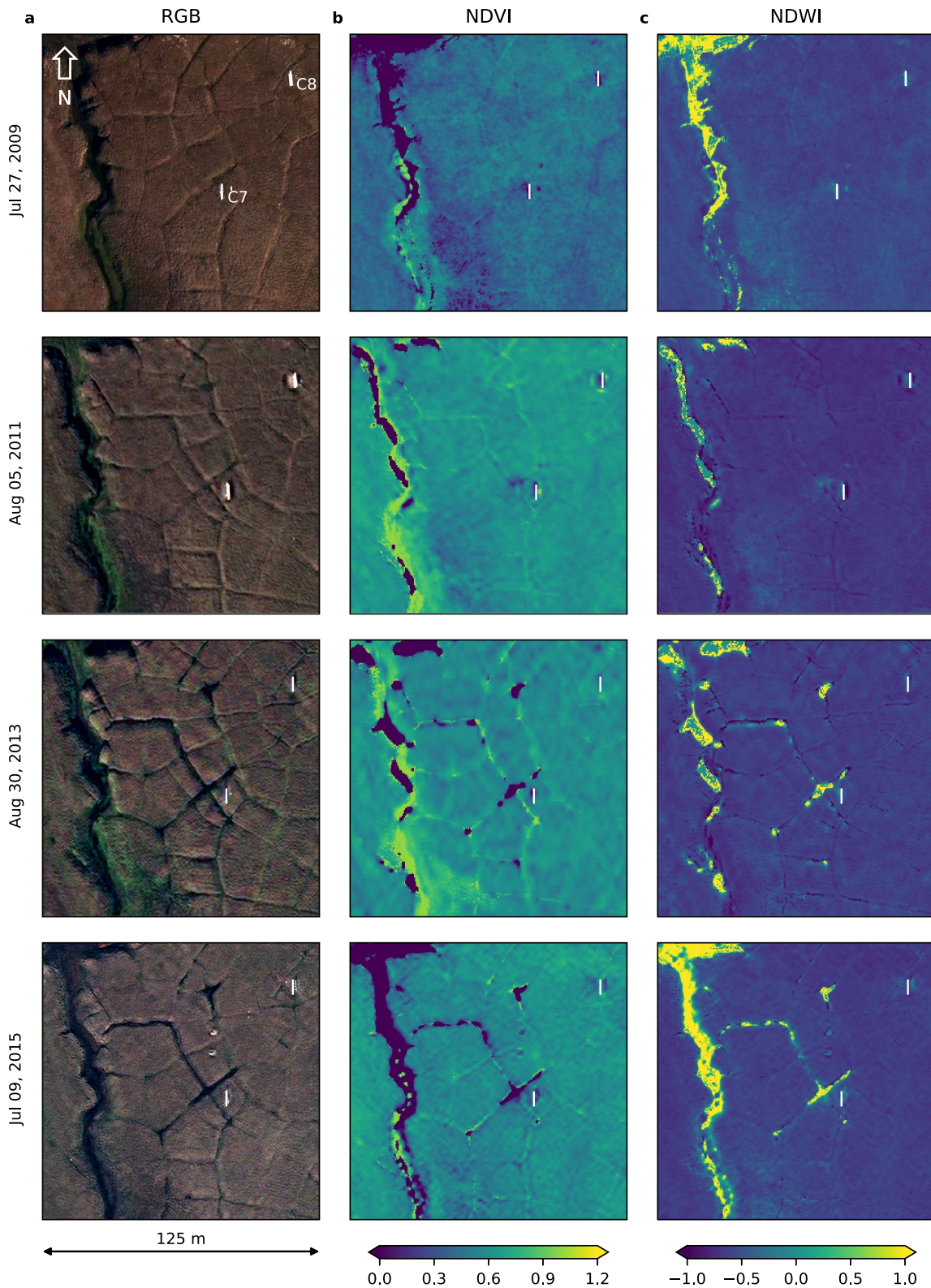


Figure 3. Chronology of ice wedge collapse in high resolution remotely sensed data. (a) Visible light imagery (RGB). The shading differs between images due to varying solar angles. (b) Normalized Difference Vegetation Index shows a large decrease west of fence C7 from 2011 to 2013, indicating less biomass. (c) Normalized Difference Water Index shows a strong increase west of fence C7 from 2011 to 2013, indicating wet conditions. The snow fences are indicated with white lines.

150 m³. If just one third of this volume consisted of sediment, rather than ice (i.e., 50 m³), and considering above-mentioned soil carbon contents, about 1.1–3.3 tons of carbon would have eroded due to the collapse of the ice wedges, although this estimate is uncertain and excludes any carbon contained in the ice itself.

4. Discussion

4.1. Climate Change Versus Snow Cover Change

Svalbard has a highly variable maritime climate, resulting in a relatively deep active layer despite its High-Arctic location (Strand et al., 2021). The archipelago also lies in the fastest warming region of the planet, with a total annual warming of ~4°C in the three decades preceding the collapse of the ice wedges (Nordli et al., 2014). This raises the question whether the observed changes are due to ambient climate change, rather than the snow fence experiment. Measurements of temperature, precipitation, and snow depth at the local airport, ~15 km away, show a large degree of interannual variation, but annual average temperatures stayed well below zero before the initial collapse of the ice wedges (Table S2 and Figure S8 in Supporting Information S1). Measurements of the active layer, ~3.5 km away in the same valley, show a thickening of 0.8 cm yr⁻¹ in response to increasing winter ground surface temperatures, but not summer warming (Schuh et al., 2017). An increase in winter-time soil temperatures is the primary climate effect that the snow fences emulate, enhancing the susceptibility of the landscape to thermokarst. Changes in the timing and thickness of snow cover can be regionally more important for permafrost warming than changes in air temperature (Biskaborn et al., 2019), and the subsidence directly behind the fences is comparable to other snow fence experiments (see e.g., Johansson et al., 2013). Moreover, subsidence due to increased snow cover has also been reported from much colder permafrost environments, for example, Northeast Siberia (Nauta et al., 2014).

In recent years, Svalbard has experienced a number of high precipitation events related to mid-winter warm spells (Hansen et al., 2014). Nonetheless, there were no other large changes in NDWI across the wider region similar to those observed near the snow fences—apart from pre-existing and seasonally varying streams (Figure S9 in Supporting Information S1). Strong subsidence was observed close to all three fences in the polygon field (Figure S3 in Supporting Information S1), while downstream effects were only observed at fence C7. This is most likely due to the fact that there were no large stream channels located up or downslope from fence C8 and C9, showing that these areas were more hydrologically isolated (Figure 2 and Figure S4 in Supporting Information S1). The formation of thermo-erosion gullies is generally not only caused by raised snow cover, but also by increased surface runoff (Godin et al., 2014). Considering all of the above, it is likely that the fast and highly localized changes observed behind, and downstream from, the C7 snow fence were primarily influenced by the experiment by accelerating the background climate change signal.

4.2. Chain of Events Triggering Permafrost Carbon Loss

The polygon troughs, acting as stream channels, are the main drainage point for the snow fence experiment, and water flowed through or remained standing in them, increasing erosion. During snowmelt, the thaw depth is still shallow and the soil is less prone to mechanical erosion from runoff (Quinton et al., 2009). However, the large amount of snow accumulated behind the fence took up to two more weeks to melt, leading to additional runoff during a time when the active layer in the downstream troughs has deepened. The deep thaw pond behind the C7 fence also acted as an additional water source—promoting channel erosion and thermal degradation (Chartrand et al., 2023). Runoff across the gullyhead may also have led to headward erosion of the polygon troughs (Fortier et al., 2007). The subsequent subsidence of the surface triggered a reinforcing mechanism: the deepening of the troughs meant that more ambient snow was trapped during winter, while concentrating runoff in summer. This raised soil temperatures even further, causing more subsidence and again deeper troughs (Figure 4). Ultimately, this led to the collapse of the ice wedges, followed by a new stable state (Figure S6 in Supporting Information S1). Gully systems can stabilize within years when well-drained and low-thermal conductivity soils develop (Fortier et al., 2007), while vegetation growth may stabilize still-intact ice wedges (Kanevskiy et al., 2017).

POC content and $\delta^{13}\text{C}$ -POC values in the gully were clearly different from the thaw ponds (Figure 2e). The terrestrial signature of gully POC suggests that this is from eroding gully walls, while POC in the thaw ponds may mostly be derived from aquatic communities, since $\delta^{13}\text{C}$ values are about -31‰ or lower (Shakil et al., 2020). The $\delta^{13}\text{C}$ values of gully DOC also clearly point toward a terrestrial source either from soil/gully erosion directly, or indirectly via leaching of particulate matter. Despite input of material in the weeks before sampling (Figure S5

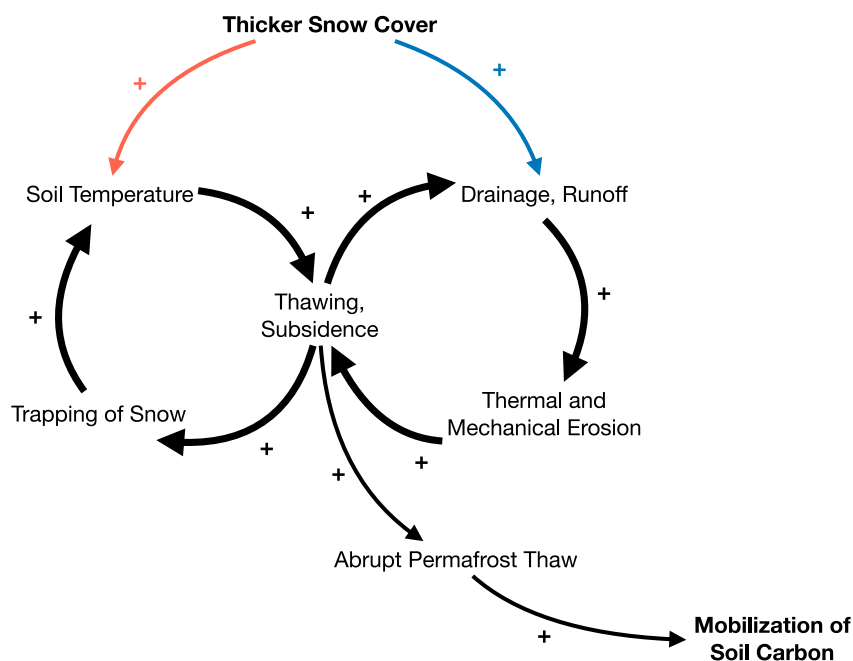


Figure 4. Thicker snow cover can trigger permafrost carbon loss through interconnected feedback loops. The red arrow indicates that thicker snow cover causes soil warming, triggering subsidence, more trapping of snow, and again more warming. The blue arrow shows how increased runoff promotes erosion, followed by subsidence, increased drainage, and again more runoff. The combined effect may ultimately trigger abrupt permafrost thaw, mobilizing soil and carbon.

in Supporting Information S1), DOC levels were lower in the gully than in the natural thaw pond (P1) and one of the two samples from behind the snow fence (F1). Together with the decrease in O_2 and increase in POC:DOC while going downstream through the gully (G1–G5), this suggests that the collapsed ice wedge is a hotspot for DOC degradation, and carbon is likely lost to the atmosphere as CO_2 . Studies from Siberia and Alaska have also shown that DOC in water originating from collapsed ice wedges is consistently more biodegradable than surface-derived DOC, and that a third can be lost within 2 weeks after thaw (Abbott et al., 2014; Vonk, Mann, Davydov, et al., 2013). In addition, we estimate that 1.1–3.3 tons of C may have eroded from the thermo-erosion gully, but parts of this soil carbon will have settled in aquatic sediments or entered the nearby fjord. The relative importance of sediment burial versus mineralization ultimately determines how much carbon mobilized by abrupt thaw processes can cascade through stream networks into the fjord (Kokelj et al., 2021), and enter the atmosphere (Vonk et al., 2015).

Ice wedges are particularly vulnerable to changes in snow cover and runoff (Godin et al., 2014), possibly enhancing permafrost carbon loss as depicted in Figure 4. Increased snow cover raises soil temperatures, which leads to subsidence in ice-rich terrain, and even more trapping of snow. Subsidence, however, also leads to a second feedback loop through enhanced drainage, thermal erosion, and further subsidence. When snow thickness increases naturally throughout the landscape, and not only locally behind snow fences, this second feedback loop is enhanced even further through increased surface runoff following snowmelt. Together, these two positive feedbacks have the potential to trigger abrupt, irreversible permafrost thaw, such as the collapse of ice wedges.

5. Conclusions

This study shows that the hydrological drainage from ice-wedge dominated permafrost environments can be highly sensitive to changes in snow thickness, not only through localized thaw subsidence and pond-formation, but also due to increased surface runoff. This can cause a collapse of ice wedges over short timescales, within a decade, triggering a loss of soil carbon that continues for years after the initial collapse through lateral export, and in situ decomposition of DOC.

Despite increases in precipitation across the Arctic, it remains uncertain how sensitive thermokarst processes are to changes in snow cover and surface runoff. Most land surface models only simulate gradual thaw, not the abrupt

thaw processes and lateral carbon flows we describe. Current projections of the strength of the permafrost carbon feedback may therefore be severely underestimated. Continued monitoring, more experimental studies, and accurate simulations of interactions with snow cover and surface runoff are urgently needed to achieve better projections of abrupt permafrost thaw and associated lateral carbon transport, and their potential to act as a positive feedback on the global climate.

Data Availability Statement

The 2009 aerial survey of the thermo-erosion gully and its surroundings is freely available copyright[©] Norwegian Polar Institute under CC BY-NC 4.0 (Norwegian Polar Institute, 2023). The satellite data from 2011, 2013, and 2015 are copyright[©] 2018 DigitalGlobe Foundation, and the processed data is available in Parmentier et al. (2024) under CC BY-NC 4.0. This public data set also includes all data from the water samples as an Excel sheet, in addition to being shown in the Table S1 in Supporting Information S1. The soil carbon data for estimating the amount of mobilized carbon are freely available from Palmtag et al. (2022) and Semenchuk et al. (2019). The weather data from Svalbard Airport, shown in Figure S8 and Table S2 in Supporting Information S1, come courtesy of the Norwegian Meteorological institute under CC BY 4.0 (MET Norway, 2024).

Acknowledgments

This research was funded by the Research Council of Norway (RCN, Grant 230970) and the FRAM—Terrestrial flagship (362255 and 642018). F.J.W.P. and S.W. received additional funding from the RCN (Grant 323945). The high-resolution satellite imagery comes courtesy of the DigitalGlobe Foundation. We thank UCLouvain and the University of California, Davis for assisting in the sample analysis.

References

- Aas, K. S., Martin, L., Nitzbon, J., Langer, M., Boike, J., Lee, H., et al. (2019). Thaw processes in ice-rich permafrost landscapes represented with laterally coupled tiles in a land surface model. *The Cryosphere*, 13(2), 591–609. <https://doi.org/10.5194/tc-13-591-2019>
- Abbott, B. W., Larouche, J. R., Jones, J. B., Bowden, W. B., & Balsler, A. W. (2014). Elevated dissolved organic carbon biodegradability from thawing and collapsing permafrost. *Journal of Geophysical Research: Biogeosciences*, 119(10), 2049–2063. <https://doi.org/10.1002/2014JG002678>
- AMAP. (2017). Snow, water, ice and permafrost in the Arctic (SWIPA) 2017 (p. xiv + 269 pp). In *Arctic monitoring and assessment programme (AMAP)*.
- Bintanja, R., & Selten, F. M. (2014). Future increases in Arctic precipitation linked to local evaporation and sea-ice retreat. *Nature*, 509(7501), 479–482. <https://doi.org/10.1038/nature13259>
- Biskaborn, B. K., Smith, S. L., Noetzli, J., Matthes, H., Vieira, G., Streletskiy, D. A., et al. (2019). Permafrost is warming at a global scale. *Nature Communications*, 10(1), 264. <https://doi.org/10.1038/s41467-018-08240-4>
- Cable, S., Elberling, B., & Kroon, A. (2018). Holocene permafrost history and cryostratigraphy in the high-Arctic Adventdalen Valley, Central Svalbard. *Boreas*, 47(2), 423–442. <https://doi.org/10.1111/bor.12286>
- Chartrand, S. M., Jellinek, A. M., Kukko, A., Galofre, A. G., Osinski, G. R., & Hibbard, S. (2023). High Arctic channel incision modulated by climate change and the emergence of polygonal ground. *Nature Communications*, 14(1), 5297. <https://doi.org/10.1038/s41467-023-40795-9>
- Cooper, E. J., Dullinger, S., & Semenchuk, P. (2011). Late snowmelt delays plant development and results in lower reproductive success in the High Arctic. *Plant Science*, 180(1), 157–167. <https://doi.org/10.1016/j.plantsci.2010.09.005>
- Cooper, E. J., Little, C. J., Pilsbacher, A. K., & Mörsdorf, M. A. (2019). Disappearing green: Shrubs decline and bryophytes increase with nine years of increased snow accumulation in the High Arctic. *Journal of Vegetation Science*, 30(5), 857–867. <https://doi.org/10.1111/jvs.12793>
- Farquharson, L. M., Romanovsky, V. E., Kholodov, A., & Nicolovsky, D. (2022). Sub-aerial talik formation observed across the discontinuous permafrost zone of Alaska. *Nature Geoscience*, 15(6), 475–481. <https://doi.org/10.1038/s41561-022-00952-z>
- Fortier, D., Allard, M., & Shur, Y. (2007). Observation of rapid drainage system development by thermal erosion of ice wedges on Bylot Island, Canadian Arctic Archipelago. *Permafrost and Periglacial Processes*, 18(3), 229–243. <https://doi.org/10.1002/ppp.595>
- Fritz, M., Opel, T., Tanski, G., Herzsuh, U., Meyer, H., Eulenburg, A., & Lantuit, H. (2015). Dissolved organic carbon (DOC) in Arctic ground ice. *The Cryosphere*, 9(2), 737–752. <https://doi.org/10.5194/tc-9-737-2015>
- Gilbert, G. L., O'Neill, H. B., Nemecek, W., Thiel, C., Christiansen, H. H., & Buylaert, J. (2018). Late Quaternary sedimentation and permafrost development in a Svalbard fjord-valley, Norwegian high Arctic. *Sedimentology*, 65(7), 2531–2558. <https://doi.org/10.1111/sed.12476>
- Godin, E., Fortier, D., & Coulombe, S. (2014). Effects of thermo-erosion gully on hydrologic flow networks, discharge and soil loss. *Environmental Research Letters*, 9(10), 105010. <https://doi.org/10.1088/1748-9326/9/10/105010>
- Hansen, B. B., Isaksen, K., Benestad, R. E., Kohler, J., Pedersen, Å. Ø., Loe, L. E., et al. (2014). Warmer and wetter winters: Characteristics and implications of an extreme weather event in the high Arctic. *Environmental Research Letters*, 9(11), 114021. <https://doi.org/10.1088/1748-9326/9/11/114021>
- Johansson, M., Callaghan, T. V., Bosjö, J., Åkerman, H. J., Jackowicz-Korczyński, M., & Christensen, T. R. (2013). Rapid responses of permafrost and vegetation to experimentally increased snow cover in sub-Arctic Sweden. *Environmental Research Letters*, 8(3), 035025. <https://doi.org/10.1088/1748-9326/8/3/035025>
- Jorgenson, M. T., Kanevskiy, M. Z., Jorgenson, J. C., Liljedahl, A., Shur, Y., Epstein, H., et al. (2022). Rapid transformation of tundra ecosystems from ice-wedge degradation. *Global and Planetary Change*, 216, 103921. <https://doi.org/10.1016/j.gloplacha.2022.103921>
- Jorgenson, M. T., & Osterkamp, T. E. (2005). Response of boreal ecosystems to varying modes of permafrost degradation. *Canadian Journal of Forest Research*, 35(9), 2100–2111. <https://doi.org/10.1139/x05-153>
- Kanevskiy, M., Shur, Y., Jorgenson, T., Brown, D. R. N., Moskalenko, N., Brown, J., et al. (2017). Degradation and stabilization of ice wedges: Implications for assessing risk of thermokarst in northern Alaska. *Geomorphology*, 297, 20–42. <https://doi.org/10.1016/j.geomorph.2017.09.001>
- Kokelj, S. V., Kokoszka, J., van der Sluijs, J., Rudy, A. C. A., Tunnicliffe, J., Shakil, S., et al. (2021). Thaw-driven mass wasting couples slopes with downstream systems, and effects propagate through Arctic drainage networks. *The Cryosphere*, 15(7), 3059–3081. <https://doi.org/10.5194/tc-15-3059-2021>
- Lachenbruch, A. H. (1962). *Mechanics of thermal contraction cracks and ice-wedge polygons in permafrost*. Geological Society of America.
- Lantuit, H., & Pollard, W. H. (2008). Fifty years of coastal erosion and retrogressive thaw slump activity on Herschel Island, southern Beaufort Sea, Yukon Territory, Canada. *Geomorphology*, 95(1–2), 84–102. <https://doi.org/10.1016/j.geomorph.2006.07.040>

- Liljedahl, A. K., Boike, J., Daanen, R. P., Fedorov, A. N., Frost, G. V., Grosse, G., et al. (2016). Pan-Arctic ice-wedge degradation in warming permafrost and its influence on tundra hydrology. *Nature Geoscience*, *9*(4), 312–318. <https://doi.org/10.1038/ngeo2674>
- MET Norway. (2024). Observations and weather statistics (station ID SN99840) [Dataset]. *Norwegian Centre for Climate Services*. Retrieved from <https://seklima.met.no>
- Natali, S. M., Schuur, E. A. G., Trucco, C., Hicks Pries, C. E., Crummer, K. G., & Baron Lopez, A. F. (2011). Effects of experimental warming of air, soil and permafrost on carbon balance in Alaskan tundra. *Global Change Biology*, *17*(3), 1394–1407. <https://doi.org/10.1111/j.1365-2486.2010.02303.x>
- Nauta, A. L., Heijmans, M. M. P. D., Blok, D., Limpens, J., Elberling, B., Gallagher, A., et al. (2014). Permafrost collapse after shrub removal shifts tundra ecosystem to a methane source. *Nature Climate Change*, *5*(1), 67–70. <https://doi.org/10.1038/nclimate2446>
- Nitzbon, J., Westermann, S., Langer, M., Martin, L. C. P., Strauss, J., Laboor, S., & Boike, J. (2020). Fast response of cold ice-rich permafrost in northeast Siberia to a warming climate. *Nature Communications*, *11*(1), 2201. <https://doi.org/10.1038/s41467-020-15725-8>
- Nordli, Ø., Przybylak, R., Ogilvie, A. E. J., & Isaksen, K. (2014). Long-term temperature trends and variability on Spitsbergen: The extended Svalbard airport temperature series, 1898–2012. *Polar Research*, *33*(1), 278. <https://doi.org/10.3402/polar.v33.21349>
- Norwegian Polar Institute. (2023). Svalbard satellite imagery [Dataset]. *Norwegian Polar Data (NP_Ortofoto_Svalbard_WMETS_3857)*. Retrieved from <https://geodata.npolar.no>
- Olefeldt, D., Goswami, S., Grosse, G., Hayes, D., Hugelius, G., Kuhry, P., et al. (2016). Circumpolar distribution and carbon storage of thermokarst landscapes. *Nature Communications*, *7*(1), 13043. <https://doi.org/10.1038/ncomms13043>
- Palmtag, J., Obu, J., Kuhry, P., Siewert, M., & Weiss, N., & Hugelius, G. (2022). Detailed pedon data on soil carbon and nitrogen for the northern permafrost region [Dataset]. *Dataset version 1. Bolin Centre Database*. <https://doi.org/10.17043/palmtag-2022-pedon-1>
- Parmentier, F.-J. W., Nilsen, L., Tømmervik, H., & Cooper, E. J. (2021). A distributed time-lapse camera network to track vegetation phenology with high temporal detail and at varying scales. *Earth System Science Data*, *13*(7), 3593–3606. <https://doi.org/10.5194/essd-13-3593-2021>
- Parmentier, F.-J. W., Nilsen, L., Tømmervik, H., Meisel, O. H., Bröder, L., Vonk, J. E., et al. (2024). Water sample analysis and satellite imagery of a thermo-erosion gully and its surroundings in Adventdalen, Svalbard. (1.0) [Dataset]. *Zenodo*. <https://doi.org/10.5281/zenodo.10991228>
- Plaza, C., Pegoraro, E., Bracho, R., Celis, G., Crummer, K. G., Hutchings, J. A., et al. (2019). Direct observation of permafrost degradation and rapid soil carbon loss in tundra. *Nature Geoscience*, *12*(8), 627–631. <https://doi.org/10.1038/s41561-019-0387-6>
- Pulliaainen, J., Luojus, K., Derksen, C., Mudryk, L., Lemmetyinen, J., Salminen, M., et al. (2020). Patterns and trends of Northern Hemisphere snow mass from 1980 to 2018. *Nature*, *581*(7808), 294–298. <https://doi.org/10.1038/s41586-020-2258-0>
- Quinton, W. L., Bemrose, R. K., Zhang, Y., & Carey, S. K. (2009). The influence of spatial variability in snowmelt and active layer thaw on hillslope drainage for an alpine tundra hillslope. *Hydrological Processes*, *23*(18), 2628–2639. <https://doi.org/10.1002/hyp.7327>
- Schostatt, M., Stibal, M., Jacobsen, C. S., Bælum, J., Taş, N., Elberling, B., et al. (2015). Distinct summer and winter bacterial communities in the active layer of Svalbard permafrost revealed by DNA- and RNA-based analyses. *Frontiers in Microbiology*, *6*, 399. <https://doi.org/10.3389/fmicb.2015.00399>
- Schuh, C., Frampton, A., & Christiansen, H. H. (2017). Soil moisture redistribution and its effect on inter-annual active layer temperature and thickness variations in a dry loess terrace in Adventdalen, Svalbard. *The Cryosphere*, *11*(1), 635–651. <https://doi.org/10.5194/tc-11-635-2017>
- Semenchuk, P. R., Christiansen, C. T., Grogan, P., Elberling, B., & Cooper, E. J. (2016). Long-term experimentally deepened snow decreases growing-season respiration in a low- and high-arctic tundra ecosystem. *Journal of Geophysical Research: Biogeosciences*, *121*(5), 1236–1248. <https://doi.org/10.1002/2015JG003251>
- Semenchuk, P. R., Krab, E. J., Hedenström, M., Phillips, C. A., Ancin-Murguzur, F. J., & Cooper, E. J. (2019). Soil organic carbon depletion and degradation in surface soil after long-term non-growing season warming in High Arctic Svalbard. *Science of the Total Environment*, *646*, 158–167. <https://doi.org/10.1016/j.scitotenv.2018.07.150>
- Shakil, S., Tank, S. E., Kokelj, S. V., Vonk, J. E., & Zolkos, S. (2020). Particulate dominance of organic carbon mobilization from thaw slumps on the Peel Plateau, NT: Quantification and implications for stream systems and permafrost carbon release. *Environmental Research Letters*, *15*(11), 114019. <https://doi.org/10.1088/1748-9326/abac36>
- Stieglitz, M., Déry, S. J., Romanovsky, V. E., & Osterkamp, T. E. (2003). The role of snow cover in the warming of arctic permafrost. *Geophysical Research Letters*, *30*(13), 149. <https://doi.org/10.1029/2003GL017337>
- Strand, S. M., Christiansen, H. H., Johansson, M., Åkerman, J., & Humlum, O. (2021). Active layer thickening and controls on interannual variability in the Nordic Arctic compared to the circum-Arctic. *Permafrost and Periglacial Processes*, *32*(1), 47–58. <https://doi.org/10.1002/ppp.2088>
- Turetsky, M. R., Abbott, B. W., Jones, M. C., Anthony, K. W., Olefeldt, D., Schuur, E. A. G., et al. (2020). Carbon release through abrupt permafrost thaw. *Nature Geoscience*, *13*(2), 138–143. <https://doi.org/10.1038/s41561-019-0526-0>
- Ulrich, M., Grosse, G., Strauss, J., & Schirmer, L. (2014). Quantifying wedge-ice volumes in Yedoma and thermokarst basin deposits. *Permafrost and Periglacial Processes*, *25*(3), 151–161. <https://doi.org/10.1002/ppp.1810>
- Vonk, J. E., Mann, P. J., Davydov, S., Davydova, A., Spencer, R. G. M., Schade, J., et al. (2013). High biolability of ancient permafrost carbon upon thaw. *Geophysical Research Letters*, *40*(11), 2689–2693. <https://doi.org/10.1002/grl.50348>
- Vonk, J. E., Mann, P. J., Dowdy, K. L., Davydova, A., Davydov, S. P., Zimov, N., et al. (2013). Dissolved organic carbon loss from Yedoma permafrost amplified by ice wedge thaw. *Environmental Research Letters*, *8*(3), 035023. <https://doi.org/10.1088/1748-9326/8/3/035023>
- Vonk, J. E., Tank, S. E., Bowden, W. B., Laurion, I., Vincent, W. F., Alekseychik, P., et al. (2015). Reviews and syntheses: Effects of permafrost thaw on Arctic aquatic ecosystems. *Biogeosciences*, *12*(23), 7129–7167. <https://doi.org/10.5194/bg-12-7129-2015>
- Zhang, X., He, J., Zhang, J., Polyakov, I., Gerdes, R., Inoue, J., & Wu, P. (2013). Enhanced poleward moisture transport and amplified northern high-latitude wetting trend. *Nature Climate Change*, *3*(1), 47–51. <https://doi.org/10.1038/nclimate1631>

References From the Supporting Information

- Morana, C., Darchambeau, F., Roland, F. A. E., Borges, A. V., Muvundja, F., Kelemen, Z., et al. (2015). Biogeochemistry of a large and deep tropical lake (Lake Kivu, East Africa: Insights from a stable isotope study covering an annual cycle. *Biogeosciences*, *12*(16), 4953–4963. <https://doi.org/10.5194/bg-12-4953-2015>